

Diffraction Characteristics of Superimposed Holographic Gratings in Planar Optical Waveguides

V. Minier, A. Kevorkian, and J. M. Xu

Abstract—We present a coupled-mode analysis of superimposed holographic transmission gratings in single-mode planar optical waveguides. The diffraction characteristics are shown to be sensitive to the polarization of the incident wave, the angular separation of the output waves and the relative index modulation between the gratings. The coupling between gratings affects the diffraction efficiencies and decreases the angular and wavelength selectivities. Nevertheless, good channel separation and high fanout can be obtained together.

RECENT developments in optical communication and integrated optics offer a new range of applications for transmission gratings in planar optical waveguides. Several types of gratings have been investigated for various applications [1]–[3]. Superimposed holographic gratings have recently been proposed for optical interconnects [4] and wavelength multiplexing or demultiplexing (WDM) [5] with promising experimental results. Basically, several gratings are sequentially recorded in a photosensitive waveguiding layer using a two-beam interference technique or an electron-beam writing technique.

Several authors have studied multiple exposed volume holographic gratings in thick emulsions using a grating decomposition approach [6] or a coupled-mode approach [7], [8] which is known to be a simple yet powerful method to describe the coupling effects in perturbed structures. In this work based on the coupled-mode theory, we will examine the coupling effects of superimposed transmission gratings on the diffraction characteristics at and near Bragg incidence in single-mode slab waveguides. Diffraction efficiency, wavelength and angular selectivity, channel separation and fanout density are discussed.

For simplicity, we consider (Fig. 1) two superimposed, index modulation type, gratings recorded in a photosensitive step-index waveguiding layer. The gratings are recorded such that they both diffract the input beam at a common input Bragg angle θ_R into two output beams at

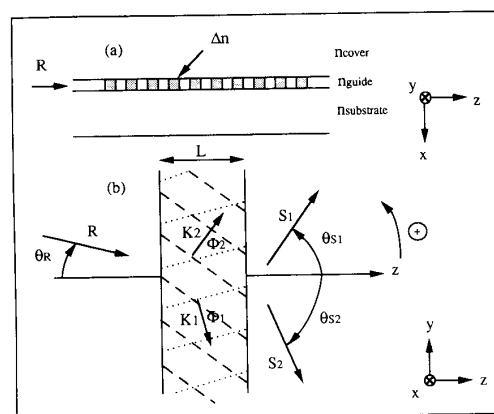


Fig. 1. Schematic structure of two superimposed holographic gratings in a step-index waveguide. Cross section (a) and top view (b).

diffraction angles θ_{S1} and θ_{S2} . We assume that the grating couplings primarily occur with one diffraction order q_i for each grating. The Bragg condition for the coplanar coupling in the guiding structure is reduced to

$$\vec{k}_{S_i} = \vec{k}_R + q_i \vec{K}_i \quad (i = 1, 2) \quad (1)$$

with k_R, k_{S_i} : wave vectors of the guided waves, ($|k_R| = |k_{S_i}| = \beta = (2\pi/\lambda)n_e$),
 K_i : grating vector of grating i ($|K_i| = 2\pi/\Lambda_i$),
 Λ_i : spatial period of grating i ,
 q_i : diffraction order related to grating i ($q_i = \pm 1, \pm 2, \dots$),
 λ : wavelength in free space,
 n_e : effective refractive index of the guided mode.

We assume a single-mode waveguiding structure so that there is no complication involving mode conversion. In fact, even for multimode structures, Nishihara [9] has shown that the TE_m - TE_n or TM_m - TM_n coupling rarely takes place in index modulation gratings and that the TE - TM coupling is considerably smaller than the primary one. Assuming that the dielectric permittivity $\epsilon(x, y, z)$ has a periodic modulation, a uniform distribution in the guiding layer and that the media is nonsaturated, the relative dielectric permittivity $\Delta\epsilon$ in the guiding layer can

Manuscript received June 8, 1992; revised July 14, 1992. This work was supported by the Ontario Laser and Lightwave Research Center (Toronto, Canada) and the Groupement d'Electromagnétisme Expérimental et d'Optoélectronique (Grenoble, France).

V. Minier and J. M. Xu are with the Department of Electrical Engineering, University of Toronto, M5S 1A4, Toronto, Canada.

A. Kevorkian is with the Groupement d'Electromagnétisme Expérimental et d'Optoélectronique, 38031, Grenoble, France.

IEEE Log Number 9203176.

be written in the Fourier decomposition:

$$\begin{aligned} \Delta\epsilon(y, z) &= \sum_{i=1}^2 \sum_{q_i=\pm 1; \pm 2..} \Delta\epsilon_{q_i} e^{-jq_i(K_i \sin \Phi_i y + K_i \cos \Phi_i z)} \\ &= \epsilon(x, y, z) - \epsilon_g \end{aligned} \quad (2)$$

with $\Delta\epsilon_{q_i}$: q th Fourier component of grating i ,
 Φ_i : slant angle of grating i ,
 ϵ_g : average dielectric permittivity in the grating region.

Following Nishihara's notations [9] and assuming $\Delta\epsilon \ll \epsilon$, the electromagnetic field distribution inside the grating region can be simplified to

$$\begin{aligned} \vec{E} &= R(z) \vec{E}_R(x, y) e^{-jk_R \cos \theta_R z} \\ &+ \sum_{i=1}^2 S_i(z) \vec{E}_{S_i}(x, y) e^{-jk_{S_i} \cos \theta_{S_i} z} \end{aligned} \quad (3)$$

with $R(z), S_1(z), S_2(z)$: amplitudes of modes along the z axis,
 $E_\mu(x, y)$: electromagnetic field distribution associated with mode μ .

The fields E_R, E_{S_1} , and E_{S_2} depend on the geometry of the guide and the polarization of the guided modes. Using this simplified field distribution, the coupled-mode equations describing the evolution of the amplitudes along z are

$$\cos \theta_\mu \frac{d}{dz} (\mu(z)) = -j \sum_\nu \kappa_{\mu\nu}(z) \nu(z) e^{-j\beta(\cos \theta_\nu - \cos \theta_\mu)z} \quad (4a)$$

with

$$\kappa_{\mu\nu}(z) = \frac{\omega\epsilon_0}{4} \int_{x'} \int_y \vec{E}_\mu^*(x, y) \Delta\epsilon(y, z) \vec{E}_\nu(x, y) dx dy. \quad (4b)$$

The term $\kappa_{\mu\nu}$ is called the coupling coefficient between modes μ and ν due to the grating perturbation. Neglecting the self-coupling terms (i.e., the small change in the propagation constant β in the grating region), substituting (1) into (4a), assuming an infinite wide grating structure along y axis, using $c_\mu = \cos \theta_\mu$ and $\Delta n_i = \Delta n_{q_i}$, these equations can be simplified to

$$\begin{aligned} c_R \frac{d}{dz} R(z) &= -j\kappa_1 e^{-j2\Delta_1 z} S_1(z) - j\kappa_2 e^{-j2\Delta_2 z} S_2(z) \\ c_{S_1} \frac{d}{dz} S_1(z) &= -j\kappa_1 e^{+j2\Delta_1 z} R(z) \\ c_{S_2} \frac{d}{dz} S_2(z) &= -j\kappa_2 e^{+j2\Delta_2 z} R(z) \end{aligned} \quad (5)$$

with $2\Delta_i = \beta c_{S_i} - (\beta c_R + q_i K_i \cos \Phi_i)$ and $\kappa_i = (\pi \Delta n_i / \lambda) C_{f_i} P_i$.

The term $2\Delta_i$ describes the deviation from the q_i th order phase-matching condition associated with the coupling of R with the grating i . The term κ_i is the simplified coupling coefficient between R and S_i . It is expressed as a function of the index modulation coefficient Δn_i of the grating i , the confinement factor C_{f_i} of the waveguide and the polarization factor P_i [9]. The confinement factor expresses how the light is confined in the waveguide. It depends on the polarization of the wave and for a well-guided mode, we can write $C_{f_i} \approx 1$. The polarization factor can be approximated by $P_i^{\text{TM}} \approx 1$ for TM-TM coupling but for the TE-TE coupling, the effect of the total diffracted angle gives $P_i^{\text{TE}} = \cos(\theta_R + \theta_{S_i})$ which becomes nil when the input and output beams are perpendicular to each other [9], [10].

For transmission gratings ($c_{S_i} > 0$), the boundary conditions are $R(0) = 1$ and $S_i(0) = 0$. With respect to energy conservation, the diffraction efficiency of each output beam is given by

$$\eta_i(z) = \frac{c_{S_i}}{c_R} |S_i(z)|^2. \quad (6)$$

At Bragg angle incidence, $2\Delta_1 = 2\Delta_2 = 0$. By integrating the simplified coupled-mode equations (5) and taking into account the boundary conditions and energy conservation, we obtain

$$\eta_i(z) = \frac{1}{1 + \left(\frac{\kappa_j}{\kappa_i}\right)^2 \frac{c_{S_i}}{c_{S_j}}} \sin^2(\sqrt{\alpha} z) \quad (7)$$

$$\text{with } \alpha = \frac{1}{c_R} \left(\frac{\kappa_1^2}{c_{S_1}} + \frac{\kappa_2^2}{c_{S_2}} \right) \text{ and for}$$

$$(i, j) = (1, 2) \text{ or } (2, 1).$$

Diffraction efficiencies exhibit the same periodic variation and achieve a first maximum for a common length $L_c = \pi/2\sqrt{\alpha}$. As shown in Fig. 2, by correctly designing the gratings, we can achieve very short gratings (staying in the Bragg regime [11]). For this purpose, input and output angles θ_R and θ_{S_i} , and coupling factors κ_i should be large. The maximum efficiency can be written (for wave S_1 for example) as

$$\eta_{1\text{max}} = \eta_1(L_c) = \frac{1}{1 + \left(\frac{\Delta n_2 P_2}{\Delta n_1 P_1}\right)^2 \frac{c_{S_1}}{c_{S_2}}}. \quad (8)$$

Again, by adjusting the same parameters as before, we can achieve maximum efficiencies between 0 and 100%. For example, Fig. 3 shows how the polarization modifies the output efficiencies, as the relative positions of the input and diffracted angles change. We can couple the same amount of energy in each beam. We can see from Fig. 3 that this condition occurs for two grating configurations for the TE polarization as it only appears once for the TM polarization.

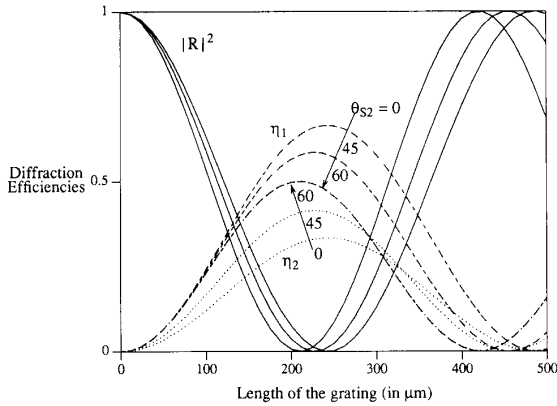


Fig. 2. Diffraction efficiencies $|R|^2$ (solid), η_1 (dashed) and η_2 (dotted) versus grating length for three beam-splitter configurations using first order diffractions ($\theta_{s2} = 0^\circ, 45^\circ, \text{ and } 60^\circ$) for a TM input wave, $\theta_R = 45^\circ$, $\theta_{s1} = 60^\circ$, $\Delta n_1 = \Delta n_2 = 1.0 \times 10^{-3}$, $\Lambda_1 = 0.41 \mu\text{m}$, $\Lambda_2 = 0.84, 0.46$ and $0.41 \mu\text{m}$, $\lambda = 1.0 \mu\text{m}$ and $n_e = 1.55$.

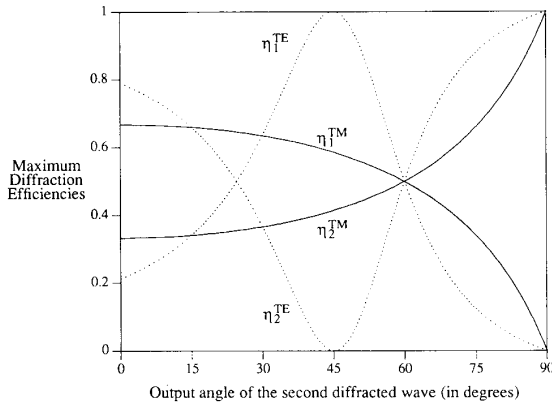


Fig. 3. Maximum diffraction efficiencies η_1^{TM} , η_2^{TM} (solid) and η_1^{TE} , η_2^{TE} (dotted) versus output angle θ_{s2} of the second diffracted wave, first order diffractions, $\theta_R = 45^\circ$, $\theta_{s1} = 60^\circ$, $\Delta n_1 = \Delta n_2 = 1.0 \times 10^{-3}$, $\Lambda_1 = 0.41 \mu\text{m}$, $\lambda = 1.0 \mu\text{m}$ and $n_e(\text{TE}) \approx n_e(\text{TM}) = 1.55$.

Near the common Bragg angle of incidence, the analytical solution becomes very involved even for only two gratings. Kowarschik developed it for thick volume holographic gratings [8]. In our work, numerical integration of the coupled mode equation system by the Runge-Kutta method has been used. We found that, as for the one grating case, both high diffraction angles and long grating structure increase the angular and wavelength selectivities. On the other hand, the strength of the second grating (index modulation) will decrease both the wavelength selectivity and the angular selectivity (Fig. 4) of the first one. For $\Delta n_2 = 0$, the solution reduces to Kogelnik's result [11] for the one grating case and for $\Delta n_2 \neq 0$, a broadening appears and becomes important for $\Delta n_2 > \Delta n_1$. Nevertheless, for close index modulations, broadening is quite small and high angular selectivities ($< 0.2^\circ$)

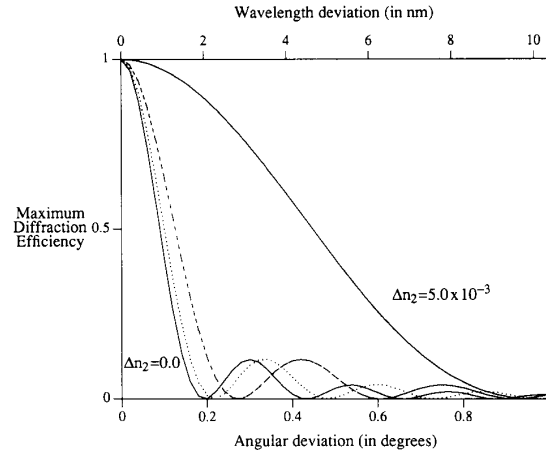


Fig. 4. Maximum diffraction efficiency $\eta_1/\eta_2(\theta_{s1})$ versus wavelength or angular deviation from the Bragg condition for a TM input wave and first order diffractions, $\theta_R = 30^\circ$, $\theta_{s1} = 60^\circ$, $\theta_{s2} = 59^\circ$, $\Delta n_1 = 1.0 \times 10^{-3}$; and $\Delta n_2 = 0$ (solid), 5.0×10^{-4} (dotted), 1.0×10^{-3} (dashed) and 5.0×10^{-3} (solid), with $\Lambda_1 = 0.45 \mu\text{m}$, $\Lambda_2 = 0.46 \mu\text{m}$, $\lambda = 1.0 \mu\text{m}$ and $n_e = 1.55$.

are preserved. Thus, a large fanout density (> 50 channels) can be expected with a good channel separation ($< 1^\circ$). A multibeam deflector 1-to-30 has already been implemented with a 2° angular separation [4].

In conclusion, superimposed holographic transmission gratings in single-mode planar optical waveguides have been investigated using coupled-mode theory. The analysis reveals that coupling between gratings not only affects diffraction efficiencies but also angular and wavelength selectivities. Diffraction efficiencies are found to greatly depend on the polarization of the propagated mode and the diffracted angles. Angular and wavelength selectivities are shown to depend on the length of the grating, the angular separation between diffracted angles and the relative strength of the gratings. Nevertheless, small channel separation can be obtained and a large channel fanout is achievable.

REFERENCES

- [1] H. Nishihara, Y. Handa, T. Suhara and J. Koyama, "Microgratings for high-efficiency guided-beam deflection fabricated by electron-beam direct-writing techniques," *Appl. Opt.*, vol. 19, pp. 2842-2847, 1980.
- [2] A. Kevorkian, "A Si integrated waveguiding polarimeter," *Proc. SPIE.*, vol. 800, pp. 98-103, 1987.
- [3] T. Suhara and H. Nishihara, "Integrated optics components and devices using periodic structures," *IEEE J. Quantum Electron.*, vol. QE-22, pp. 845-867, 1986.
- [4] M. R. Wang, G. J. Sonek, R. T. Chen, and T. Jansson, "Large fanout optical interconnects using thick holographic gratings and substrate wave propagation," *Appl. Opt.*, vol. 31, pp. 236-249, 1992.
- [5] W. Liu, E. Strzelecki, and T. Jansson, "High resolution integrated optic holographic wavelength division multiplexer," *Proc. SPIE.*, vol. 1635, pp. 20-24, 1990.
- [6] R. Alferness and S. K. Case, "Coupling in doubly exposed, thick holographic gratings," *J. Opt. Soc. Amer.*, vol. 65, pp. 730-739, 1975.
- [7] S. K. Case, "Coupled-wave theory for multiply exposed thick holographic gratings," *J. Opt. Soc. Amer.*, vol. 65, pp. 724-729, 1975.

- [8] R. Kowarschik, "Diffraction efficiency of sequentially stored gratings in transmission volume holograms," *Optica Acta.*, vol. 25, pp. 67-81, 1978.
- [9] H. Nishihara, M. Haruna, and T. Suhara, *Optical Integrated circuits*. New York: McGraw-Hill, 1991, ch. 3, 4.
- [10] K. Wagatsuma, H. Sakaki, and S. Saito, "Mode conversion and optical filtering of obliquely incident waves in corrugated waveguide filters," *IEEE J. Quantum Electron.*, vol. QE-15, pp. 632-637, 1979.
- [11] H. Kogelnik, "Coupled wave theory for thick hologram gratings," *Bell Syst. Tech. J.*, vol. 48, pp. 2909-2947, 1969.

A Wide-Angle Vector Beam Propagation Method

W. P. Huang and C. L. Xu

Abstract—A wide-angle vector beam propagation method is developed and presented. Considerable improvement in accuracy over the paraxial vector propagating algorithms is achieved with virtually no additional computation.

THE conventional beam propagation methods (BPM) [1], [2] solve scalar wave equations under paraxial approximation and hence apply only to simulation of scalar wave propagation along waveguide axis in weakly guiding structures. Several numerical algorithms to treat the vectorial wave propagation (vector BPM) have been reported recently [3]–[5]. The VBPM's are capable of simulating polarized or even hybrid wave propagation in strongly guiding structures. One of the shortcomings of the current VBPM's is that the paraxial approximation is still assumed in the governing equations and only waves propagating close to the waveguide axis may be accurately predicted. In the strongly guided structures, guided modes may be formed by bouncing waves propagating at large angles with the waveguide axis. Even for weakly guided structures, radiation caused by longitudinal index perturbations may occur at large angles off the waveguide axis. Furthermore, a reference refractive index must be assumed in all the paraxial (scalar and vector) propagating algorithms. The choice of the reference index is critical for the accuracy of the numerical solutions. Although an optimum reference index may be obtained by a modal calculation [5], to determine the optimum refractive index in practice is cumbersome and difficult in practical applications.

Manuscript received May 18, 1992; revised July 7, 1992. This work was supported in part by the grant from the Natural Science and Engineering Research Council of Canada. C. L. Xu acknowledges the post-graduate scholarship from the Natural Science and Engineering Research Council of Canada.

The authors are with the Department of Electrical and Computer Engineering, University of Waterloo, Waterloo, Ont., Canada N2L 3G1. IEEE Log Number 9203174.

A number of propagating algorithms to overcome the paraxial approximation have been developed in various fields [6] and introduced to guided-wave optics [7], [8]. One of the schemes based on the Pade approximation presented by Hadley [8] demonstrates considerable improvement over the paraxial BPM's. A similar algorithm is developed in this letter for the vectorial wave propagation. This is, to our knowledge, the first wide-angle vectorial propagating algorithm (wide-angle VBPM) reported so far.

If the refractive index varies slowly along z and the reflections due to the longitudinal variation of the refractive index can be neglected, the propagation of the electromagnetic waves is governed by the vector wave equation for the electric field

$$\left(1 + j \frac{1}{2n_o k} \frac{\partial}{\partial z}\right) \frac{\partial}{\partial z} E_x = -jA_{xx} E_x \quad (1a)$$

$$\left(1 + j \frac{1}{2n_o k} \frac{\partial}{\partial z}\right) \frac{\partial}{\partial z} E_y = -jA_{yy} E_y \quad (1b)$$

where $k = \omega\sqrt{\epsilon_o\mu_o}$ and $n = n(x, y, z)$ is the refractive index of the medium. A time dependence of $e^{j\omega t}$ has been assumed. The parameter n_o is a reference refractive index and should be chosen to be close to the weighted average of the effective index of the structure. The differential operators are defined by

$$A_{xx} E_x = \frac{1}{2n_o k} \left\{ \frac{\partial}{\partial x} \left[\frac{1}{n^2} \frac{\partial}{\partial x} (n^2 E_x) \right] + \frac{\partial^2}{\partial y^2} E_x + (n^2 - n_o^2) k^2 E_x \right\} \quad (2a)$$

$$A_{yy} E_y = \frac{1}{2n_o k} \left\{ \frac{\partial^2}{\partial x^2} E_y + \frac{\partial}{\partial y} \left[\frac{1}{n^2} \frac{\partial}{\partial y} (n^2 E_y) \right] + (n^2 - n_o^2) k^2 E_y \right\}. \quad (2b)$$